6
UNSTEADY FLOW IN PIPES

6.1 Introduction

Unsteady flow in pipes results primarily from the operation of flow regulation devices such as valves or pumps. Its practical significance is due to the fact that the associated pressure changes may exceed the permitted value or fluctuation range for the pipe material. Such transient pressures are dependent on a number of factors, including the rate of acceleration or deceleration of the fluid, the compressibility of the fluid, the elasticity of the pipe and the overall geometry of the pipe system.

The audible noise sometimes associated with unsteady pipe flow is often described as "waterhammer", due to the hammer-like sound sometimes emitted as a result of vapour pocket collapse or pipe vibration. The basic equations which describe unsteady flow in pipes are developed by applying the principles of continuity and momentum to a control volume, as illustrated on Fig 6.1. These basic equations together with appropriate boundary condition equations, define the flow regime and their solution allows the prediction of the variation of dependent variables, pressure (p) and flow velocity (v) with independent variables, time (t) and location (x).

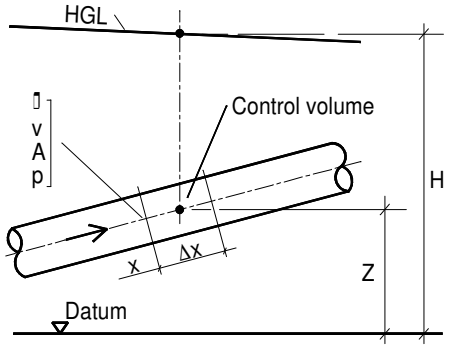

Fig 6.1 Control volume definition

6.2 The continuity equation

The continuity or mass balance equation is developed for the flow length ∂x:

Mass inflow rate - mass outflow rate = rate of change of contained mass

$$\rho A v - \left\{ \rho A v + \frac{\partial}{\partial x}(\rho A v)\partial x \right\} = \frac{\partial}{\partial t}(\rho A \partial x) \qquad (6.1)$$

where A is the pipe cross-sectional area and ρ is the fluid density. Simplifying (6.1), we get

$$\frac{\partial}{\partial x}(\rho A v)\partial x + \frac{\partial}{\partial t}(\rho A \partial x) = 0$$

Hence

$$v\frac{\partial}{\partial x}(\rho A)+\rho A\frac{\partial v}{\partial x}+\frac{\partial}{\partial t}(\rho A)=0$$

since

$$\frac{\partial}{\partial t}(\rho A)=v\frac{\partial}{\partial x}(\rho A)+\frac{\partial}{\partial t}(\rho A)$$

Hence

$$\rho A\frac{\partial v}{\partial x}+\frac{d}{dt}(\rho A)=0$$

$$\rho A\frac{\partial v}{\partial x}+A\frac{d\rho}{dt}+\rho\frac{dA}{dt}=0 \qquad (6.2)$$

The change in fluid density is a function of the increase in pressure and the fluid bulk modulus. By definition the bulk modulus K = dp/(-dV/V), where V is volume. Density and volume change are related thus: $-dV/V = d\rho/\rho$. Hence, the following correlation of density change with pressure change: $d\rho = (\rho/K)dp$. The change in pipe cross-sectional area is a function of the change in fluid pressure, the wall thickness of the pipe T, and the Young's modulus E of the pipe material. The change in area $dA = 2\pi R\, dR = (2A/R)dR$, where R is the pipe radius. The increase in radius $dR = (dp\, R^2)/TE$; hence $dA = dp(AD/TE)$, where D is the pipe diameter.

Equation (6.2) may therefore be written as follows:

$$\rho A\frac{\partial v}{\partial x}+\frac{A\rho}{K}\frac{dp}{dt}+\frac{\rho AD}{TE}\frac{dp}{dt}=0$$

$$\rho\frac{\partial v}{\partial x}+\frac{dp}{dt}\left(\frac{\rho}{K}+\frac{\rho D}{TE}\right)=0$$

$$\rho\frac{\partial v}{\partial x}+\frac{1}{\alpha^2}\frac{dp}{dt}=0$$

where

$$\alpha=\frac{1}{\sqrt{\rho/K+\rho D/TE}}$$

Hence

$$\rho\frac{\partial v}{\partial x}+\frac{\rho g}{\alpha^2}\left(\frac{\partial H}{\partial x}v+\frac{\partial H}{\partial t}-\frac{\partial Z}{\partial x}v-\frac{\partial Z}{\partial t}\right)=0 \qquad (6.3)$$

where $p = \rho g(H - Z)$ and $\frac{dp}{dt}=v\frac{\partial p}{\partial x}+\frac{\partial p}{\partial t}$

Equation (6.3) can be written in the form

$$\frac{\partial H}{\partial t}+v\frac{\partial H}{\partial x}-v\sin\theta+\frac{\alpha^2}{g}\frac{\partial v}{\partial x}=0 \qquad (6.4)$$

This is the desired form of the continuity equation. α Is the speed of propagation of a pressure wave through the pipe; its magnitude is dependent on two factors, the bulk modulus of the fluid K and the rigidity of the pipe, as measured by the ratio TE/D. The expression for α may be modified to take into account the Poisson effect on pipe expansion and the influence of pipe anchorage conditions (Wylie & Streeter, 1978) :

$$\alpha=\frac{1}{\sqrt{\rho/K+\rho CD/TE}} \qquad (6.5)$$

where C is an anchorage coefficient with values as follows:

(1) pipe anchored at upstream end only: $C = 1-\mu/2$;
(2) pipe anchored throughout against axial movement $C = 1-\mu^2$
(3) pipe with expansion joints: $C = 1$

where μ is Poisson's ratio for the pipe material.

The practical range of wavespeed encountered in the water engineering field varies from about 1400 ms^{-1} for small diameter steel pipes to about 280 ms^{-1} for low pressure PVC pipes, with intermediate values for pipes in materials such as asbestos cement and concrete (Creasey et al, 1977). A small amount of free gas (i.e. undissolved gas) has a considerable influence on wavespeed, effecting a reduction in wavespeed as the pressure drops and the gas volume expands (Wylie & Streeter, 1978). A free gas phase can arise from air intake through air valves or from air release from solution during negative gauge pressure or from the biological production of gases in wastewaters.

6.3 The momentum equation

The force/momentum relation is applied to the fluid contained in the control volume defined in Fig 6.1:

$$pA - \left(pA + \frac{\partial}{\partial x}(pA)\partial x \right) - \tau_0 \pi D dx - \rho g A \partial x \sin\theta = \frac{dv}{dt}(\rho A \partial x) \qquad (6.6)$$

Simplifying:

$$\frac{\partial}{\partial x}(pA) + \tau_0 \pi D + \rho g A \sin\theta + \rho A \frac{dv}{dt} = 0 \qquad (6.7)$$

where τ_0 is the wall shear stress = $\rho g R_h S_f$, R_h being the hydraulic radius = D/4 and S_f being the friction slope = $f v|v|/2gD$. Expressing pressure in terms of H and Z, equation (6.8) may be written in the form

$$\frac{\partial(H-z)dx}{\partial x} + S_f + \sin\theta + \frac{1}{g}\frac{dv}{dt} = 0$$

or

$$\frac{\partial H}{\partial x} - \frac{\partial Z}{\partial x} + \frac{fv|v|}{2gD} + \sin\theta + \frac{1}{g}\left(v\frac{\partial v}{\partial x} + \frac{\partial v}{\partial t} \right) = 0$$

Hence

$$g\frac{\partial H}{\partial x} + v\frac{\partial v}{\partial x} + \frac{\partial v}{\partial t} + \frac{fv|v|}{2D} = 0 \qquad (6.8)$$

which is the desired form of the momentum equation. Note that $|v|$ means the absolute value of v. In expanding the term $\partial(pA)/\partial x$, it has been assumed that $\partial A/\partial x$ can be neglected; also $\partial Z/\partial x = \sin\theta$.

6.4 Solution by the method of characteristics

A general solution to the above pair of partial differential equations (variables v, H, x, t) is not available. They can, however, be transformed by the method of characteristics into a set of total differential equations which can be integrated to finite difference form for convenient solution by numerical methods. Note that v and H are the dependent variables, while x and t are the independent variables.

For ease of solution the two equations can be simplified by omitting the less important terms as follows:

the continuity equation

$$\frac{\partial H}{\partial t} + v\frac{\partial H}{\partial x} - v\sin\theta + \frac{\alpha^2}{g}\frac{\partial v}{\partial x} = 0$$

becomes

$$\frac{\partial H}{\partial t} + \frac{\alpha^2}{g}\frac{\partial v}{\partial x} = 0 \qquad (6.9)$$

the momentum equation

$$g\frac{\partial H}{\partial x} + v\frac{\partial v}{\partial x} + \frac{\partial v}{\partial t} + \frac{fv|v|}{2D} = 0$$

becomes

$$g\frac{\partial H}{\partial x} + \frac{\partial v}{\partial t} + \frac{fv|v|}{2D} = 0 \qquad (6.10)$$

Multiplying equation (6.90) by a factor λ and adding to equation (6.10):

$$\lambda\left(\frac{g}{\lambda}\frac{\partial H}{\partial x} + \frac{\partial H}{\partial t}\right) + \frac{\lambda a^2}{g}\frac{\partial v}{\partial x} + \frac{\partial v}{\partial t} + \frac{fv|v|}{2D} = 0$$

which can be written in total differential form as follows:

$$\lambda\frac{dH}{dt} + \frac{dv}{dt} + \frac{fv|v|}{2D} = 0 \qquad (6.11)$$

provided that

$$\frac{dx}{dt} = \frac{g}{\lambda} = \frac{\lambda a^2}{g}$$

hence $\lambda = \pm g/\alpha$, so

$$\frac{dx}{dt} = \pm\alpha \qquad (6.12)$$

Equations (6.11) and (6.12) are the equivalent total differential forms of the partial differential continuity and momentum equations. They can be written as two linked pairs of equations ('characteristic equations') as follows:

$$+\frac{g}{\alpha}\frac{dH}{dt} + \frac{dv}{dt} + \frac{fv|v|}{2D} = 0 \qquad (6.13)$$

C^+

$$\frac{dx}{dt} = +\alpha \qquad (6.14)$$

$$-\frac{g}{\alpha}\frac{dH}{dt} + \frac{dv}{dt} + \frac{fv|v|}{2D} = 0 \qquad (6.15)$$

C^-

$$\frac{dx}{dt} = -\alpha \qquad (6.16)$$

Equations (6.14) and (6.16) are graphically represented as straight lines on the x-t plane, as illustrated on Fig 6.2. Equations (6.13) and (6.15) define the variations of H and v with time subject to the x-t relationships of equations (6.14) and (6.16), respectively.

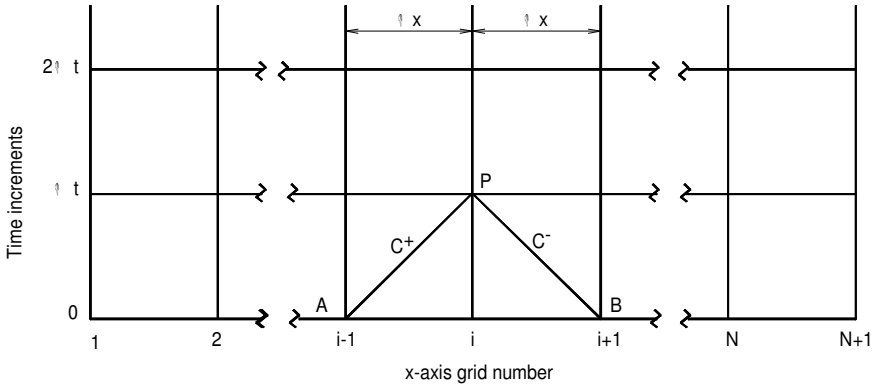

Fig 6.2 The x-t finite difference grid

6.4.1 Finite difference formulations

The pipeline is divided into N reaches, each of length Δx, from which the computational time step Δt is calculated:

$$\Delta t = \frac{\Delta x}{\alpha} \tag{6.17}$$

Integrating equation (6.13) along the C^+ characteristic:

$$\int dH + \frac{\alpha}{g}\int dv + \frac{\alpha f}{2gD}\int v|v|dt = 0$$

Replacing v by Q/A:

$$\int dH + \frac{\alpha}{gA}\int dQ + \frac{\alpha f}{2gDA^2}\int Q|Q|dt = 0$$

Integration over the interval Δx:

$$H_p - H_A + \frac{\alpha}{gA}(Q_P - Q_A) + \frac{f\Delta x}{2gDA^2}Q_A|Q_A| = 0 \tag{6.18}$$

Similarly for the C^- characteristic equations:

$$H_p - H_B - \frac{\alpha}{gA}(Q_P - Q_B) - \frac{f\Delta x}{2gDA^2}Q_B|Q_B| = 0 \tag{6.19}$$

Equations (6.18) and (6.19) can be written as

C^+: $$H_P = H_A - B(Q_P - Q_A) - RQ_A|Q_A| \tag{6.20}$$

C^- $$H_P = H_B + B(Q_P - Q_B) + RQ_B|Q_B| \tag{6.21}$$

where

$$B = \frac{\alpha}{gA} \qquad \text{and} \qquad R = \frac{f\Delta x}{2gDA^2}$$

Thus if H_A, Q_A, H_B and Q_B are known, the values of H_P and Q_P can be calculated by solution of equations (6.20) and (6.21). Referring to the x-t plane, note the displacement in space and time of P from A and B.

Equations (6.20) and (6.21) can be written in grid reference form as follows:

$$C^+: \qquad H_{Pi} = H_{i-1} - B\left(Q_{Pi} - Q_{i-1}\right) - RQ_{i-1}|Q_{i-1}| \qquad (6.22)$$

$$C^-: \qquad H_{Pi} = H_{i+1} + B\left(Q_{Pi} - Q_{i+1}\right) + RQ_{i+1}|Q_{i+1}| \qquad (6.23)$$

Assembling known values together:

$$H_{i-1} + BQ_{i-1}RQ_{i-1}|Q_{i-1}| = CP$$

$$H_{i+1} - BQ_{i+1} + RQ_{i+1}|Q_{i+1}| = CM$$

Equations (6.22) and (6.23) can thus be written as follows:

$$H_{Pi} = CP - BQ_{Pi} \qquad (6.24)$$

$$H_{Pi} = CM + BQ_{Pi} \qquad (6.25)$$

Solving for H_{Pi} and Q_{Pi}:

$$H_{Pi} = \frac{CP + CM}{2} \qquad (6.26)$$

$$Q_{Pi} = \frac{CP - CM}{2B} \qquad (6.27)$$

Thus the computation procedure uses the current values of H and Q at points i-1 and i+1 to compute their values at point i at one time interval Δt later. Usually, the starting values are known from a prevailing prior steady flow condition.

6.5 Boundary conditions

In general, waterhammer results from a sudden change in the operational mode of a flow control device such as a pump, valve or turbine. These devices may be located at either end of a pipeline or at some intermediate point. If the control is at the downstream end (x=L), the C^+ characteristic equation can be used, while if at the upstream end, the C^- characteristic equation can be applied. The second equation in each case is provided by the H/Q relation for the control device itself. The following are typical boundary condition equations.

6.5.1 **Reservoir**

1. At upstream end of the line:

C^- characteristic: $Hp_1 = CM + BQ_{P1}$

Boundary condition: $H_{P1} = H_R$

where H_R is the fixed reservoir head. Hence, compute Q_{P1}.

2. At the downstream end of the line:

C^+ characteristic: $H_{P(N+1)} = CP - BQ_{P(N+1)}$

Boundary condition $H_{P(N+1)} = H_R$.

Hence, compute $Q_{P(N+1)}$. This is illustrated in Fig 6.3.

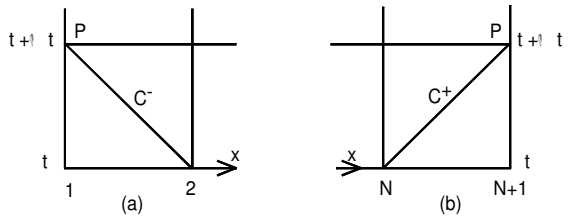

Fig 6.3 Reservoir boundary: (a) upstream end; (b) downstream end.

6.5.2. **Pump at the upstream end (running at fixed speed)**

As already shown in Chapter 5, the characteristic head-discharge curve for a fixed speed rotodynamic pump can be expressed as follows:

$$h_p = A_0 + A_1 Q + A_2 Q^2 \qquad (5.9)$$

where A0 is the shut-off head, A_1 and A_2 are constant coefficients. Taking the water level in the pump sump as reference datum and neglecting losses in the suction line, the relevant equations may be written as follows:

C^- characteristic: $H_{P1} = CM + BQ_{P1}$
Pump boundary condition: $H_{P1} = A_0 + A_1 Q_{P1} + A_2 Q^2_{P1}$

Solution of these equations yields the following:

$$Q_{P1} = \frac{1}{2A_2}\left[B - A_1 + \sqrt{(B - A_1)^2 + 4A_2(CM - A_0)}\right]$$

$$H_{P1} = A_0 + A_1 Q_{P1} + A_2 Q^2_{P1}$$

6.5.3. **Control valve at downstream end**

As indicated in chapter 5, the head loss h_v across a valve may be expressed in the form

$$H_v = K_v Q^2 \qquad (5.7)$$

where K= is a valve coefficient, the value of which may be computed from the valve K-values given in Table 3.5.

The downstream boundary condition equations thus become

C^+ characteristic: $H_{P(N+1)} = CP - BQ_{P(N+1)}$

Valve flow: $$Q_{P(N+1)} = \sqrt{\frac{H_{P(N+1)}}{K_v}}$$

where the downstream valve level is taken as datum, and there is a free discharge; where the discharge is to a fixed level reservoir, the reservoir level is taken as datum.

Solution of these two equations for Q yields the following:

$$Q_{P(N+1)} = -\frac{B}{2K_v} + \sqrt{\frac{1}{4}\left(\frac{B}{K_v}\right)^2 + \frac{CP}{K_v}}$$

Knowing $Q_{P(N+1)}$, $H_{P(N+1)}$ is found from the C^+ characteristic equation.

The special case of a closed valve or 'dead end' at the downstream end of a pipeline is found from the foregoing equations by giving K_v an infinite value, resulting in the following expression for H and Q:

$$H_{P(N+1)} = CP$$

$$Q_{P(N+1)} = 0$$

6.5.4. **Valve at an intermediate location**

The upstream side of the valve is denoted by the subscript i and the downstream side by the subscript i+1, as shown on Fig 6.4.

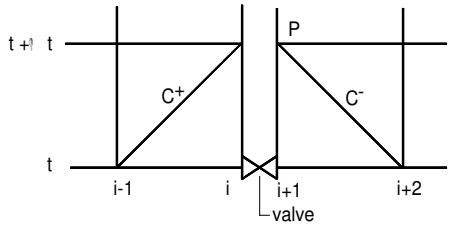

Fig 6.4 **Internal valve**

The defining equations are:

C^+ characteristic: $H_{Pi} = CP - BQ_{Pi}$

C^- characteristic: $H_{P(I+1)} = CM + B_{QP(I+1)}$

Valve flow: $$Q_{Pi} = \sqrt{\frac{H_{Pi} - H_{P(i+1)}}{K_v}}$$

Continuity: $Q_{Pi} = Q_{P(I+1)}$

Solution of these four equations for Q yields:

$$Q_{Pi} = -\frac{B}{K_v} + \sqrt{\left(\frac{B}{K_v}\right)^2 - \frac{CM - CP}{K_v}}$$

Hence H_{Pi} and $H_{P(i+1)}$ can be found from the C^+ and C^- characteristic equations, respectively.

6.5.5. **Change in pipe size**

Assuming the junction is at node i, as illustrated on Fig 6.5, the following equations apply:

C^+ characteristic: $H_{Pi} = CP_1 - B_1 Q_{Pi}$

C^- characteristic: $H_{Pi} = CM_2 + B_2 Q_{PI}$

Hence

$$Q_{Pi} = \frac{CP_1 - CM_2}{B_1 + B_2}$$

where the subscript 1 refers to pipe 1 and the subscript 2 refers to pipe 2, respectively. It should be noted that the pipe length between node points will not be the same in the two pipes if their wavespeeds differ, since this length $\Delta x = \Delta t/\alpha$, where α is the wavespeed.

The same approach can be applied to any other change in pipe properties and can also be extended to pipe junctions.

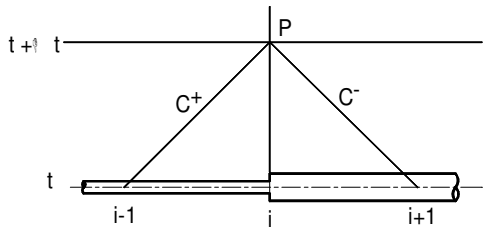

Fig 6.5 **Change in pipe size**

6.6 **Pressure transients due to pump starting and stopping**

The start-up and stopping of pumps give rise to rapid change in pipeline velocity and hence waterhammer effects. This is particularly so in pump cut-out due to power failure. This latter condition must be evaluated in all pumping installations to ensure that pressures are contained within permissible value ranges.

6.6.1 **Pump characteristics**

This discussion is confined to pumps of the rotodynamic type. The performance of rotodynamic pumps is defined for a normal or rated speed in terms of the parameters h_R, Q_R , N_R and T_R , referring to head, discharge, speed and torque, respectively. The values of these parameters at any other speed N can be related to the rated values as follows:

$$\frac{Q_N}{Q_R} = \frac{N}{N_R}; \qquad \frac{h_N}{h_R} = \frac{N^2}{N_R{}^2}; \qquad \frac{T_N}{T_R} = \frac{N^2}{N_R{}^2} \tag{6.28}$$

The torque-discharge pump characteristic may be expressed in a quadratic form similar to head-discharge equation:

$$T = B_0 + B_1 Q + B_2 Q^2 \tag{6.29}$$

By applying the homologous relationships of (6.28) to the head-discharge and torque-discharge equations, the following expressions for pump head and pump torque, at any speed N, are found:

$$h_N = A_0\left(\frac{N}{N_R}\right)^2 + A_1\left(\frac{N}{N_R}\right)Q + A_2 Q^2 \tag{6.30}$$

$$T_N = B_0\left(\frac{N}{N_R}\right)^2 + B_1\left(\frac{N}{N_R}\right)Q + B_2 Q^2 \tag{6.31}$$

When a pump motor cuts out, the inertia of the rotating parts maintains a decreasing pump output in accordance with the deceleration relationship:

$$T = -I\frac{d\omega}{dt} \tag{6.32}$$

where T is the reactive torque of the fluid, I is the moment of inertia of the rotating elements of the pump set, $-d\omega/dt$ is the angular deceleration. Thus

$$d\omega = -\frac{T}{I}dt$$

or

$$dN = -\frac{60}{2\pi}\frac{T_N}{I}dt \tag{6.33}$$

where N is the rotational speed in rpm. The pump characteristics at the reduced speed can be determined from the rated values using the relationships (6.30) and (6.31).

6.6.2 **Pump cut-out: governing equations for pump node**

The pump node is illustrated on Fig 6.6. The pump operational condition being considered is deceleration under zero external power input. The governing equations are as follows:

C^+ characteristic: $H_{Pi} = CP - BQ_{Pi}$

C^- characteristic: $H_{P(I+1)} = CM + BQ_{P(I+1)}$

Pump discharge: $H_{P(I+1)} - H_{Pi} = h_N$

Continuity: $Q_{Pi} = Q_{P(i+1)}$

where h_N is the pump manometric head at pump speed N, as expressed by equation (6.30).

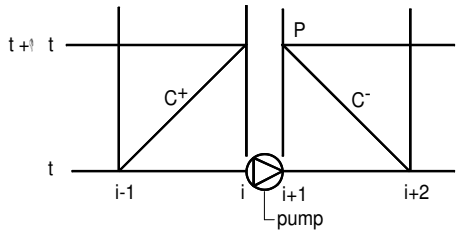

Fig 6.6 **Pump boundaries**

Simultaneous solution of the above equations gives the following value for Q_{Pi}:

$$Q_{Pi} = \frac{-(A_{1N} - 2B) + \sqrt{(A_{1N} - 2B)^2 - 4A_2(A_{0N} - CM + CP)}}{2A_2}$$

where $A_{1N} = A_1(N/N_R)$ and $A_{0N} = A_0(N/N_R)^2$. Knowing Q_{Pi}, H_{Pi} and $H_{P(I+1)}$ can be determined from the foregoing C^+ and C^- characteristic equations. The step change in N for each time interval Δt is found from eqn (6.33). The value of T_N for any Q and N is found from eqn (6.31).

6.7 Waterhammer control

The most frequently encountered waterhammer problems in water engineering relate to (a) abrupt pump stopping, as in power failure and (b) rapid valve closure. Practical control devices, which can be used to limit the waterhammer effects due to pump cutout, include the following:

(1) Use of a flywheel to increase the pumpset inertia

(2) Installation of an air vessel or accumulator

(3) Surge tank

(4) Air valves

6.7.1 **Flywheel**

The increased inertia provided by a flywheel extends the stopping time of a pump (eqn. 6.32) and hence reduces waterhammer. Its effect is computed by simply adding the flywheel inertia to that of the pumpset.

6.7.2 **Air vessel**

Air vessels are frequently used on pump rising mains for the control of transient pressures. They are typically located close to the pump, downstream of the non-return valve, as shown on Fig 6.7.

When the pump stops, the delivery pressure immediately drops, causing a rapid discharge from the air vessel and immediate closure of the non-return valve (NRV). In the associated waterhammer analysis it is usually assumed that closure of the non-return valve is instantaneous and coincident with pump stopping, hence the air vessel becomes the effective upstream boundary control.

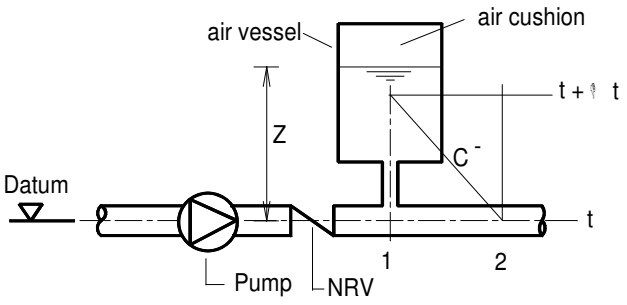

Fig 6.7 **Air vessel boundary**

The governing equations are as follows:

C^- characteristic:	$H_{P1} = CM + BQ_{P1}$
Air volume/head:	$h_a V_a^{\gamma} = \text{constant}$
Throttle head loss:	$h_L = C\,Q_{P1}^2$
h_a/H_{P1} relation:	$h_a = H_{P1} + H_{atm} + h_L - Z$
Continuity:	$\Delta V = 0.5\Delta t(Q_{P1} + Q_1)$

where h_a is the absolute pressure head, H_{atm} is the atmospheric pressure head, C is a head loss coefficient for flow between the air vessel and the rising main - generally the throttle is designed to have a lesser head loss during outflow from the air vessel than during flow into the vessel, resulting in different C-values for inflow and outflow. The air volume change occurs rapidly and hence closely approximates an adiabatic process (γ = 1.4 for air). A γ-value of 1.35 is recommended for practical flow computations.

The above equations are solved for H_{P1} and Q_{P1}; initially, Q_1 may be assumed to be zero. The values of Z and V_a are modified for the next time step as follows:

$$Z_{t+\Delta t} = Z_t - \frac{\Delta t\left(Q_{P1} + Q_1\right)}{2A_v}$$

$$V_{a(t+\Delta t)} = V_{a(t)} + 0.5\Delta t\left(Q_{P1} + Q_1\right)$$

where A_v is the cross-sectional area of the air vessel.

The air cushion functions rather like a spring, expanding during periods of water outflow from the vessel and thus exerting an increasing restraining force on the water outflow, eventually causing flow reversal. The resulting inflow to the vessel causes a compression of the enclosed gas volume, which in turn exerts an increasing flow-resisting force. The natural frequency of the corresponding water mass oscillation is much lower than that of the waterhammer wave, which also travels back and forth along the pipe and is superimposed on the mass oscillation.

6.7.3 **Surge tank**

Surge tanks are open-top vessels connected to the pipe system in which pressure transients are to be controlled. They are similar to air vessels, differing in the respect that the overlying air pressure

remains constant. They give rise to a similar mass oscillation under transient flow conditions. They are often used in hydropower plants, as illustrated on Fig 6.8.

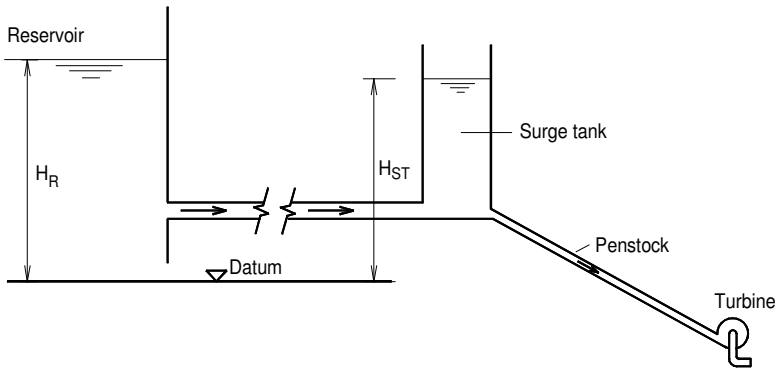

Fig 6.8 Reservoir – surge tank system

When flow to the turbine is throttled back, the penstock is subjected to waterhammer transient pressure. The surge tank prevents these transients from reaching the supply main connecting the reservoir to the surge tank. This system may be analysed using the waterhammer equations already presented. Alternatively, the transient behaviour of the reservoir-pipe-surge tank part of the system can be modelled as a simple mass oscillation:

Momentum equation: $$\rho g\left(H_R - H_{ST}\right)A - \rho g h_f A = \rho AL\frac{\Delta v}{\Delta t}$$

Continuity: $$\Delta H_R = -\frac{Q\Delta t}{A_R} \quad \text{and} \quad \Delta H_{ST} = \frac{Q\Delta t}{A_{ST}}$$

Where h_f is the flow head loss between the reservoir and the surge tank, A_R and A_{ST} are the reservoir and surge tank plan areas, respectively, and A is the pipe cross-sectional area.

This set of equations can be solved numerically to determine the variation of H_R and H_{ST} with time, resulting from an abrupt change in flow to the turbine.

6.7.4 **Air valves**

Air valves are installed at high points on rising mains to allow escape of air. They also admit air when the gauge pressure drops below atmospheric pressure and hence can be used to limit the pressure downsurge under waterhammer conditions.

6.8 Column separation, entrained gas

Column separation occurs when the pressure drops to vapour level resulting in the formation of a vapour cavity which grows in size as long as the pressure remains below vapour level. When the pressure rises the vapour cavity collapses, resulting in a high pressure at the cavity location due to the collision of two water masses moving in opposite directions. The resulting collision pressure head rise is

$$\Delta H = \frac{\alpha}{2gA}\left(Q_u - Q\right)$$

where Q_u is the inflow to the section and Q is the outflow. While analytical procedures, which take vapour formation into account, are available (Wylie & Streeter, 1978), computed and observed pressure levels do not always show good agreement. From a design viewpoint, as later discussed, it is good practice to control pressure transients so as to avoid vapour pocket formation.

Dissolved gases are released from solution when the water pressure drops below their solution pressure. The rate of release of dissolved air depends on the saturation excess and the degree of turbulence in the flow. The primary effect of a dispersed gas phase is to reduce the wavespeed, in accordance with the following correlation (Wylie and Streeter, 1978)

$$\alpha = \sqrt{\frac{1}{\rho_L(1/K_L + D/ET + mR\Theta/p^2)}} \qquad (6.34)$$

where

m is the mass of gas per unit volume of fluid,
R is the specific gas constant,
Θ is the absolute temperature (K),
p is the absolute pressure
the subscript L indicates denotes liquid phase parameters.

Equation 6.34 assumes an isothermal expansion of the gas phase which is assumed to have a low volumetric fraction. Fig 6.9 shows the quantitative influence of entrained air and pressure on wavespeed.

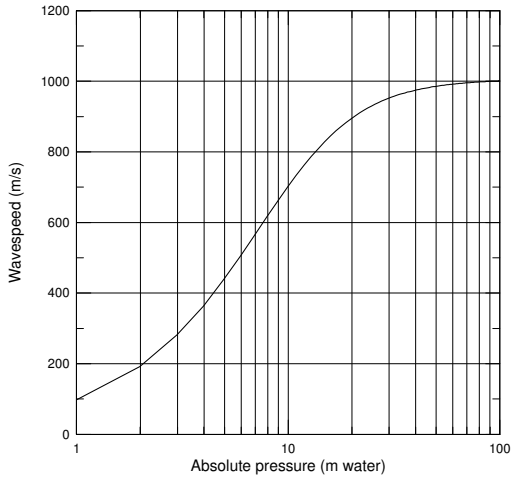

Fig 6.9 **The influence of entrained air on wavespeed**
Entrained air 0.01% by volume at an absolute pressure of 1 bar and temperature 20 ^{o}C.

It is worth noting that wastewaters such as raw sewage may have sufficient entrapped gases of biological origin to significantly reduce the waterhammer wavespeed. Conditions favourable to the production of biogases exist in sewage rising mains of low gradient and low pumping velocity, resulting in permanent organic solids deposition.

The expulsion of entrapped air, following pump start-up or filling of a pressure main, may sometimes give rise to severe pressure transients. This would happen, for example, where a main is charged rapidly

with water at one end while the contained air is displaced through an air valve at the other end. The rapidly moving water column will be halted abruptly as the air valve closes once the pipe is completely filled with water. This problem can be avoided by a gradual charging of empty mains.

In general, however, the presence of a dispersed gas phase tends to suppress waterhammer effects.

6.9 Transient pressure limits

As a general rule, specifications permit a maximum transient pressure during waterhammer conditions, which is in excess of the permissible maximum sustained working pressure. In addition, pipes which are vulnerable to fatigue failure, notably prestressed concrete and plastics, have a limiting value for the maximum pressure fluctuation (max. - min.), which is permitted under waterhammer conditions.

For cast iron, ductile iron, steel and asbestos cement pressure pipes it is generally recommended (BS 8010, Pt. 2, 1987) that the maximum pressure due to waterhammer should not exceed the maximum permissible sustained working pressure by more than 10 per cent.

For prestressed concrete it is recommended (Creasey & Sanderson 1977) that (a) the maximum pressure under waterhammer conditions not exceed the maximum permissible sustained working pressure by more than 20% and (b) the maximum pressure fluctuation amplitude not exceed 40% of the maximum permissible sustained working
pressure.

For uPVC pipe it is recommended (BSI, CP 312, 1973) that (a) the maximum pressure under waterhammer conditions not exceed the maximum permissible sustained working pressure and (b) the maximum pressure fluctuation amplitude not exceed 50% of the maximum permissible sustained working pressure and (c) Class B pipe should not be used where the pressure, under waterhammer conditions, is likely to fall below atmospheric pressure.

Where analysis indicates that the pressure is likely to drop to vapour level and thus cause column separation, it is generally advisable to install some form of waterhammer control to either prevent such cavitation from occurring or to curtail the resulting pressure transients to predictable limits.

6.10 Computer software: ARTS

The ARTS hydraulic design software developed by Aquavarra Research Limited incorporates an unsteady flow analysis capability for pump/rising main systems, due to sudden pump cut-out, using the analytical procedures set out in this chapter. The software is coded to deal with a system bounded by fixed level reservoirs at the upstream and downstream ends. The analysis presumes a non-return valve on the pump delivery. Provision is also made for the optional inclusion of an air vessel in the system. The air vessel is connected to the rising main by a throttle pipe on the downstream side of the non-return valve.

The user may therefore choose to analyse the system with the air vessel included or omitted. In the absence of an air vessel, the analysis assumes that the non-return valve closes simultaneously with the occurrence of zero forward flow in the rising main. As discussed later, this may not always happen in practice. Valve closure may not occur until there is a significant reverse velocity through the valve, resulting in more severe transient pressures than predicted by analysis (refer Fig 6.14).

Where the system includes an air vessel, the non-return valve is assumed to close simultaneously with pump cut-out and hence the air vessel becomes the effective upstream boundary of the system. In most practical cases, the suction main is very much shorter than the rising main. The rising main is divided into a number of segments (10 or a multiple thereof). The corresponding segmental length for the suction main is calculated and, if found to be greater than the actual suction main length, the latter is

defined as "short". In this circumstance the suction main pressure is assumed to remain constant and its piezometric head value is taken to correspond with the suction reservoir level.
The required input data includes the following:

PIPES: length, diameter, surface roughness, wall thickness, Young's modulus for pipe material.

PUMPS: head/discharge and power/discharge characteristics, rated speed, moment of inertia of pump set.

AIR VESSEL: volume of vessel, air volume in vessel under steady flow conditions, throttle pipe details, air vessel cross-sectional area, height of water in vessel above connection point to the rising main.

RESERVOIRS: water surface elevation relative to piezometric head datum.

A graphical representation of the system is constructed by the user on the computer screen, selecting the system components from the ARTs tool palette. The appropriate data, as listed above, are assigned to each component in the system. The head/discharge and power/discharge characteristics for the pump or pumps are defined from the use of three points on the respective characteristic curves.

6.11 **Examples of waterhammer computation**

The computed results in the examples which follow are presented in graphical form as (a) envelopes of the maximum and minimum pressures experienced over the pipe length and (b) the variation of discharge and pressure with time at the point of origin of the waterhammer effect.

Example 1 illustrates computed waterhammer pressure fluctuation due to pump trip-out and shows the effect of installing air vessel protection in reducing pressure oscillation. Example 2 illustrates the waterhammer effects of valve closure.

Example 1

Example is a typical small pump/rising main system, which delivers drinking water from a low level reservoir or sump to a high level reservoir, as illustrated in Fig 6.10. The waterhammer condition analysed is that caused by pump trip-out.

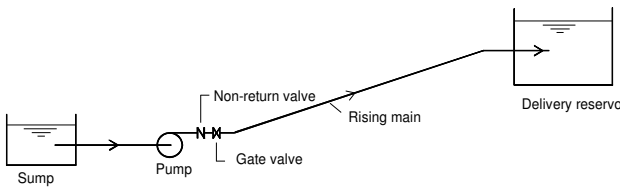

Fig 6.10 Schematic layout of pump/rising main system

System data:

Pump:	Single duty pump with standby unit.	
	H/Q curve presented in Fig 6.10a.	
	Speed (rpm)	2850
	Moment of inertia (mkg^2)	0.10
Rising main:	Medium density polyethylene	
	Length (m)	599
	Internal diameter (mm)	158.8
	Pipe wall thickness (mm)	10.6
	Young's modulus for pipe material ($N\ m^{-2}$)	$0.8x10^9$
Sump TWL (mOD)		72.10
Delivery reservoir TWL (mOD)		102.6

Steady flow conditions

The steady flow pump duty point is plotted in Fig 6.10a, where it is defined by the intersection of the head/discharge curves for the pump and rising main system, respectively.

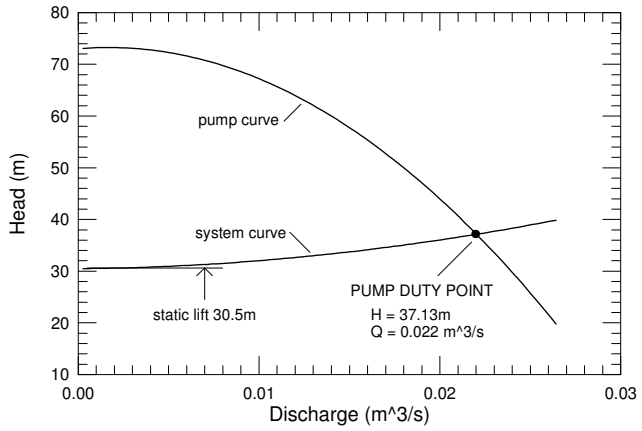

Fig 6.10a Computation of pump duty point

Pump trip-out

The computed pressure transient limits resulting from a sudden trip-out of the duty pump are plotted in Fig 6.10b, which includes the following:

1. the rising main profile
2. the maximum and minimum pressure envelopes following pump trip-out
3. the steady flow hydraulic gradient line (HGL)
4. vapour pressure limit line

The pressure graphs are plotted as potential head (mOD) and hence the gauge pressure at any point is the vertical difference between the plotted pressure line and the rising main elevation at that point.

The results plotted in Fig 6.10b show an upsurge in gauge pressure from a steady flow value of 35.0m to a peak value of 52.5m at the pump end of the rising main. The plotted results also show a negative gauge pressure over a 260m length of the rising main, dropping to a minimum value of about –8.0m at a point some 450m from the pump end of the main.

The generation of sub-atmospheric pressure can be eliminated by the connection of an air vessel to the rising main, downstream of the non-return valve at the pump end of the main. Fig 6.10c shows the impact of such an installation on the transient pressures resulting from pump trip-out. The plotted pressure envelopes for the protected system show that the pressure upsurge is reduced while the pressure downsurge is reduced, thereby eliminating negative gauge pressure.

The temporal variations in pressure at the pump end of the protected rising main, following pump trip-out, with and without air vessel protection, are plotted on Fig 6.10d. For the unprotected system, the frequency of the oscillation reflects the return travel time of the waterhammer pressure wave. For the air vessel system, the pressure oscillation reflects the mass oscillation of the water contained in the rising main in response to the expansion and contraction of the compressed air cushion contained in the air vessel.

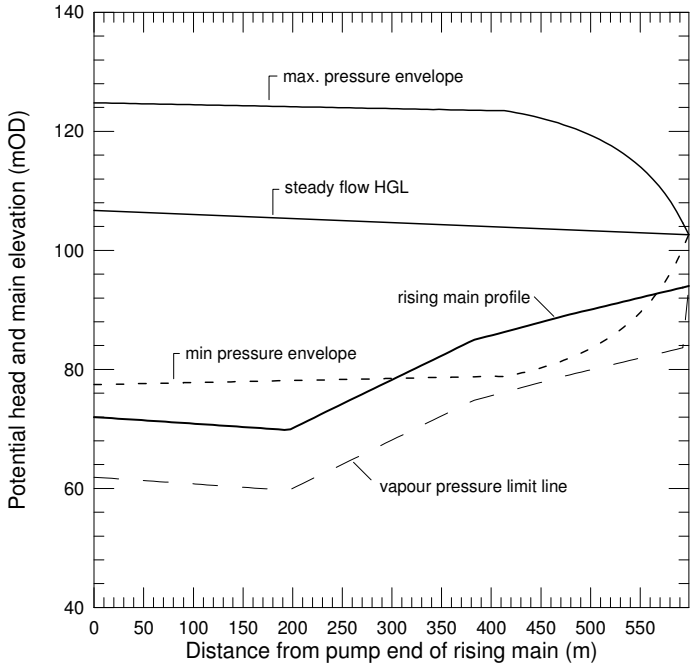

Fig 6.10b Pressure envelopes for pump trip-out condition

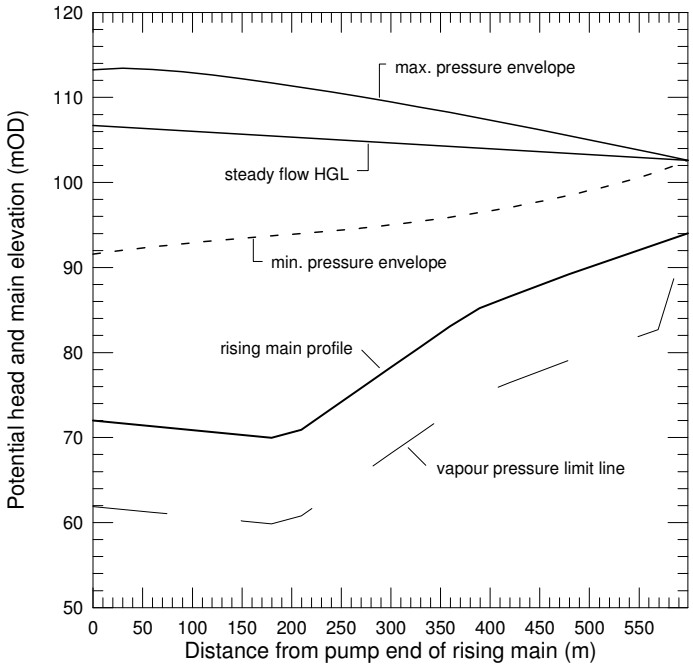

Fig 6.10c Pressure envelopes for system protected by an air vessel
Vessel gross volume 0.5m^3; air volume at steady flow 0.25m^3;
Connecting throttle pipe diameter 150mm.

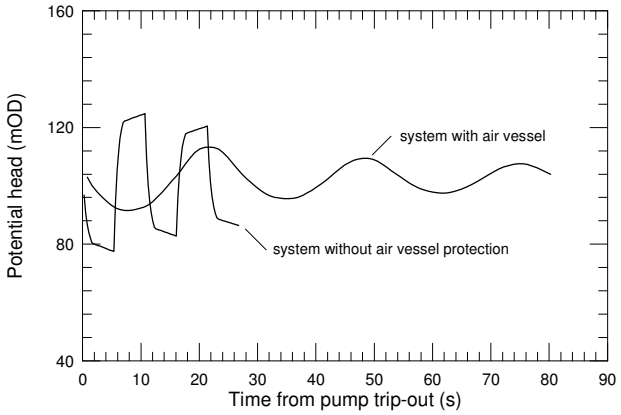

Fig 6.10d Temporal pressure fluctuation at pump end of rising main following pump trip-out.

Example 2

Example 2 illustrates the transient flow conditions caused by valve closure. Valve closure causes a deceleration of flow, which may give rise to a significant transient pressure fluctuations if the rate of deceleration is high, as would be caused by rapid valve closure.

Fig 6.13 shows a gravity flow pipeline connecting two reservoirs separated by a distance of 2.5 km. The pipeline has a butterfly valve at its midpoint. When such a valve is closed, it generates transient flow conditions upstream and downstream of the valve. The magnitude of the pressure fluctuation depends on the rate of valve closure.

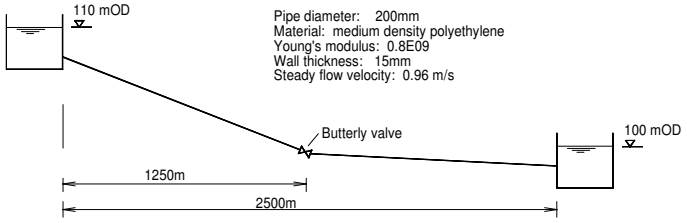

Fig 6.13 **Pipeline schematic**

Fig 6.13(a) shows the computed pressure fluctuations on the upstream and downstream sides of the valve as the valve disc is rotated through 90^o from the fully open to the fully closed position for two closures routines:

(1) closure at a uniform rate of 1^o per second, resulting in a closure time of 90 seconds;
(2) 2-step closure routine, the initial closure rate being 2^o per second over the first 60^o of disc rotation followed by a rate of 0.5^o per second over the final 30^o of disc rotation, also giving a closure time of 90 seconds.

As may be seen from the valve K-values presented in Table 3.5, the flow regulation impact of butterfly valves is effectively confined to the final 45^o of disc rotation. This valve characteristic is reflected in the plotted pressure fluctuations in Fig 6.13a, which show that the pressure drop across the valve due to the initial 45^o of closure is relatively minor (ca. 0.5m).

The plotted results indicate that the maximum upsurge pressure on the upstream side of the valve for the uniform closure rate is about 13m, with a corresponding downsurge of equal magnitude on the downstream side of the valve. The maximum upsurge pressure on the upstream side of the valve for the 2-step closure rate is about 7m, with a corresponding downsurge of equal magnitude on the downstream side of the valve. This example illustrates the feasiblity of designing a multi-step automatic valve closure routine, to achieve closure in a minimum time while not exceeding the permissible pressures for the pipe system. Such valve closure optimisation is known as valve stroking (Streeter, 1963).

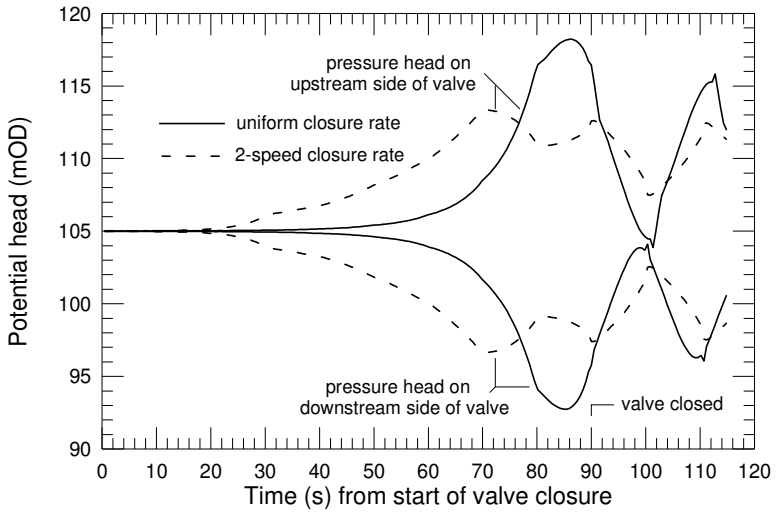

Fig 6.13a Computed pressures on the upstream and downstream sides of the valve shown on Fig 6.13, due to the closure rates indicated in the text

6.12 Some practical design considerations

In practical pipeline design in respect of waterhammer effects it is the obvious goal of the designer to ensure that pressure extremes remain within permissible limits, as previously outlined. Where the analysis indicates that cavitation is likely to occur, appropriate design steps should, as a general rule, be taken to eliminate the possibility of vapour pocket formation because of the risks associated with vapour pocket collapse. This will usually be achieved by the use of air valves or an air vessel or other control device appropriate to the prevailing circumstances.

It is also good practice to verify, where possible, analytical predictions by post-installation field measurements, particularly where there is a degree of uncertainty in the predicted response of the system under investigation. The measurement of waterhammer pressure transients requires a fast-response pressure-sensing device such as a piezoresistive transducer, linked to a compatible recording system.

Figs 6.14 and 6.15 illustrate recorded pressure transients in which the system response was found to differ significantly from that which would be predicted from conventional analysis of the respective systems.

Fig 6.14 shows measured transient pressure traces following pump trip-out on a laboratory test rig rising main. The relevant rising main data were as follows: low-density polyethylene pipe, 150 m long, 50 mm diameter. The steady flow forward velocity was 1.25 ms^{-1} and the static lift was 6.0 m. The rising main was fitted with a standard hinged flap non-return valve (NRV) on the delivery side of the pump.

Pressure traces 1 and 2 show the recorded pressure transients, following pump trip-out, at a point just downstream of the NRV. Prior to the recording of pressure trace 2 the NRV flap was spring-loaded so as to make its closure coincide with the reduction of the forward velocity to zero value? The delayed closure of the NRV (the time duration from pump cut-out to the first rising leg of pressure trace 1 was about 3s longer than the corresponding time for pressure trace 2) is clearly seen to cause a dramatic jump in the maximum positive waterhammer pressure, raising the piezometric value from about 9.0m to about 25.0m. This increase in pressure is due to the fact that the delayed closure of the NRV flap allowed a significant reverse velocity to develop prior to closure. The instantaneous stoppage of this reverse flow, as the flap closed, gave rise to the observed increase in peak transient pressure. The sharp impact of closure under such circumstances typically produces an audible valve-slam sound.

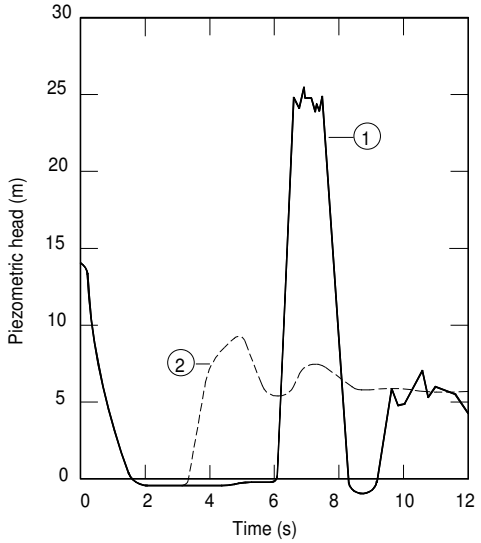

Fig 6.14 Measured pressure traces following pump trip-out; (1) is unmodified NRV and (2) is spring-loaded NRV (Purcell 1991, personal communication).

Fig 6.15 shows a measured waterhammer pressure trace, recorded on the downstream side of the non-return valve on a rising main. As the system data given on Fig 6.15 indicates, the pump/rising main

system belongs in the same category as the system analysed in example 1, i.e. it is a short rising main in which the friction head is small relative to the static lift. The measured pressure variation with time is generally similar to that computed for example 1, as presented on Fig 6.10 (b). There are, however, a number of significant differences. The computed wavespeed for this rising main was 1153 ms^{-1} , resulting in an estimated wave return travel time of 0.32s; the measured return travel time was 0.75s, indicating an actual average wavespeed of 493 ms^{-1} . This low wavespeed is indicative of the presence of dispersed gas bubbles in the pumped liquid, which was municipal sewage. As there was no possibility of air entry to the system or air release from solution, it was concluded that the gas phase was of biological origin.

A second notable feature of the measured pressure trace is the pronounced damping in the system as is evident from the decrease in magnitude of successive pressure peaks. This decrease is much higher than predicted by the usual computational assumption that flow friction under waterhammer conditions is the same as in steady flow at the same velocity. This is clearly not the case; it would appear that the effective energy dissipation under conditions of rapid velocity change is significantly higher than that which obtains under steady flow conditions.

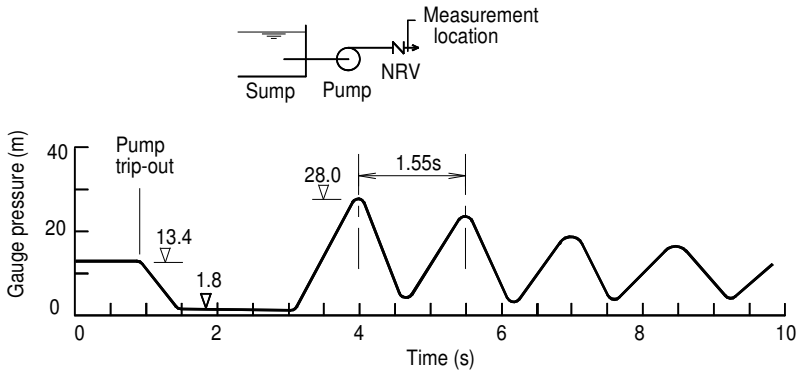

Fig 6.15 Measured pressure trace following pump trip-out. Experimental results: maximum head rise = 14.6m; maximum head drop = 11.6m. The graph is for a cast iron rising main 185m long with an internal diameter of 389mm; discharge rate = 0.100 m^3s^{-1}; static lift = 12.7m; friction head = 0.67m.

6.13 **Some relevant material properties**

Bulk modulus of water (K) = 2.05×10^9 Nm^{-2}

Vapour pressure of water

Temperature (^oC)	Vapour pressure (mm water)
5	89
10	125
15	174
20	239
25	323

Young's modulus (E) for pipe materials

Material	Young's modulus (10^{10} Nm^{-2})
Cast iron	11.2
Ductile iron	15.0
Steel	20.0
Copper	11.5
Asbestos cement	2.5
Prestressed concrete	3.7
uPVC	0.3
Polyethylene	0.08
ABS	0.17
Perspex	0.6
Nylon	0.2

REFERENCES

British Standards Institution (1973). BS 8010, Part 2, 1987;CP312, Part 2.

Chaudry, M. Hanif (1987) Applied Hydraulic Transients, 2nd. Edn, van Nostrand Rheinhold Co., New York.

Creasey, J. D. and Sanderson, P. R. (1977). Surge in water and sewage pipelines, TR 51, Water Research Centre, Medmenham, U.K.

Streeter, V. L. (1963) Valve stroking to control waterhammer. Jour. Hyd. Div. ASCE, 89, pp. 39-66.

Wylie, E. B. and Streeter, V. L. (1978). Fluid Transients, McGraw Hill International Book Co., New York.